engineering proceedings

MDPI

Proceeding Paper

A Framework for Extending Simu5G with Nakagami-*m* and *κ*-*μ* Fading Models †

Ricardo Mena Villacis [1,*], Jhonny Ruiz Vacas [2], Luis Urquiza-Aguiar [2], José Vega-Sánchez [3] and Mónica Aguilar Igartua [1]

[1] Department of Network Engineering, Universitat Politècnica de Catalunya (UPC), 08034 Barcelona, Spain; monica.aguilar@upc.edu
[2] Departamento de Electrónica, Telecomunicaciones y Redes de Información (DETRI), Escuela Politécnica Nacional, Quito 170143, Ecuador; jhonny.ruiz@epn.edu.ec (J.R.V.); luis.urquiza@epn.edu.ec (L.U.-A.)
[3] Colegio de Ciencias e Ingenierías "El Politécnico", Universidad San Francisco de Quito (USFQ), Quito 170157, Ecuador; dvega@usfq.edu.ec
* Correspondence: ricardo.mena@upc.edu
† Presented at the XXXIV Conference on Electrical and Electronic Engineering (JIEE 2026), Quito, Ecuador, 26–30 October 2026.

Abstract

System-level evaluation of fifth-generation (5G) vehicular networks requires channel models for diffuse fading and dominant propagation components. Simu5G provides a simulation environment based on the Objective Modular Network Testbed in C++ (OMNeT++) and the INET Framework (INET) for 5G New Radio (NR) studies, but its current fading workflow includes only Rayleigh- and Jakes-type behavior. This paper integrates configurable Nakagami-*m* and *κ*-*μ* processes into the channel model and background-interference processing paths. The extension adds Network Description (NED) language parameters and attenuation functions while preserving the fadingType interface. Verification combines Monte Carlo distributions with simulator exports for single-vehicle and 100-vehicle runs. For $m = 2$, $\Omega = 1$, $\kappa = 2$, and $\mu = 2$, the probability of normalized fading gain below −10 dB is 0.0953 for Rayleigh, 0.0825 for Jakes, 0.0177 for Nakagami-*m*, and 0.0045 for *κ*-*μ*. System-level traces show effects on the signal-to-interference-plus-noise ratio (SINR), channel quality indicator (CQI), and throughput. The implementation enables controlled generalized-fading studies and provides a reproducible basis for more conclusive system-level performance evaluations.

Keywords: Simu5G; OMNeT++; 5G NR; V2X; vehicular networks; Nakagami-*m*; *κ*-*μ*; channel modeling; system-level simulation

1. Introduction

Fifth-generation (5G) vehicular systems require reproducible evaluation of propagation, mobility, scheduling, protocols, and traffic that field trials alone cannot provide. Simu5G, built on the Objective Modular Network Testbed in C++ (OMNeT++) and INET Framework (INET), models 5G New Radio (NR) access, core data planes, mobility, and end-to-end applications, including cellular vehicle-to-everything (C-V2X) scenarios [1,2].

Network conclusions depend on physical-layer assumptions. Vehicular links exhibit Doppler effects, blockage, clustered scattering, specular components, and rapid line-of-sight (LOS)/non-line-of-sight (NLOS) transitions [3,4]. Rayleigh represents diffuse scattering, whereas the Jakes sum-of-sinusoids construction adds temporal correlation

Check for updates

Published: 2 November 2026

Copyright: © 2026 by the authors. Licensee MDPI, Basel, Switzerland. This article is an open access article distributed under the terms and conditions of the Creative Commons Attribution (CC BY) license.

but can exhibit finite-realization artifacts and cannot generally parameterize clustered dominant components [5–7].

Nakagami-m controls fading severity and includes Rayleigh power at $m = 1$ [8]; κ-μ represents scattered and dominant components across effective multipath clusters [9]. This flexibility suits vehicle-to-everything (V2X) links, where propagation regimes vary and link adaptation maps channel variation into channel quality indicator (CQI), throughput, and reliability changes [10,11].

Recent studies demonstrate Simu5G extensibility and generalized fading relevance [12–15]. Analytical families include λ-κ-μ for correlated components, its double form for cascaded links, α-η-μ/IGA for nonlinear shadowed multipath, and log-λ-κ-μ for low-altitude UAV channels [16–19]. This work instead closes a system-level implementation gap by translating configurable Nakagami-m and κ-μ behavior into Simu5G's native channel, interference, and V2X workflow.

The contribution is therefore a configurable Simu5G extension that preserves the existing interface while broadening the propagation conditions available for system-level evaluation.

2. Channel Models

2.1. Rayleigh and Jakes Baselines

Let R denote the envelope of a zero-mean complex Gaussian channel, with variance σ^2 per quadrature component. The Rayleigh probability density function (PDF) is

$$f_R(r) = \frac{r}{\sigma^2} \exp\left(-\frac{r^2}{2\sigma^2}\right), \qquad r \geq 0. \tag{1}$$

The Jakes model is not a separate fading distribution: it is a temporally correlated Rayleigh process constructed through a finite sum of sinusoids (SoS), whose Doppler shifts depend on the maximum Doppler frequency and selected angles of arrival [5]. Therefore, the Rayleigh and Jakes curves share the same target marginal distribution and differ in their temporal correlation and finite-realization behavior. Their comparison in this study is used only to distinguish independent Rayleigh sampling from the existing temporally correlated Jakes implementation.

2.2. Nakagami-m Fading

For Nakagami-m fading, the envelope R has the probability density function (PDF) [8]

$$f_R(r) = \frac{2m^m}{\Gamma(m)\Omega^m} r^{2m-1} \exp\left(-\frac{m}{\Omega} r^2\right), \qquad r \geq 0. \tag{2}$$

Here, $m \geq 1/2$ controls fading severity and $\Omega > 0$ is the mean received power. Consequently, the instantaneous received power $P = R^2$ follows a Gamma distribution [8], i.e.,

$$P \sim \Gamma\left(m, \frac{\Omega}{m}\right). \tag{3}$$

Values $1/2 \leq m < 1$ represent fading more severe than Rayleigh, $m = 1$ yields the Rayleigh power law, and $m > 1$ produces a less dispersed envelope.

2.3. κ-μ Fading

The κ-μ model describes μ effective multipath clusters with a dominant-to-scattered power ratio κ. A normalized envelope PDF is [9]

$$\begin{aligned} f_R(r) = {} & \frac{2\mu(1+\kappa)^{(\mu+1)/2}}{\kappa^{(\mu-1)/2}\Omega^{(\mu+1)/2}\exp(\mu\kappa)} r^{\mu} \exp\left[-\frac{\mu(1+\kappa)}{\Omega} r^2\right] \\ & \times I_{\mu-1}\left(2\mu r\sqrt{\frac{\kappa(1+\kappa)}{\Omega}}\right), \qquad r \geq 0, \end{aligned} \tag{4}$$

https://doi.org/10.3390/engproc2026158006

where $I_{\mu-1}(\cdot)$ is the modified Bessel function of the first kind. Increasing κ strengthens dominant propagation components, while increasing μ generally reduces the relative fluctuation produced by any single cluster.

3. Materials and Methods

3.1. Simu5G Integration

The extension targets the Simu5G folders named `channelmodel` and `cell`. The modified files identified in the retained implementation record are:

- `LteRealisticChannelModel`: `.ned`, `.h`, `.ini`, and `.cc`;
- `NrChannelModel_3GPP38_901.cc`;
- `BackgroundCellChannelModel`: `.ned`, `.h`, and `.cc`.

The Network Description (NED) interface extends the existing selector and exposes the model parameters:

```
string fadingType @enum(RAYLEIGH,JAKES,KAPPAMU,NAKAGAMI)
                  = default("JAKES");
double kappa = default(2.0);
int mu = default(2);
double nakagamiM = default(2.0);
double nakagamiOmega = default(1.0);
```

C++ enumerations and state variables store parameters read once at initialization, while SINR, reference signal received power, and background-interference paths dispatch to the selected function. The new identifiers in `NrChannelModel_3GPP38_901.cc` prevent Third Generation Partnership Project (3GPP) TR 38.901 configurations from rejecting the models before attenuation evaluation [20,21].

3.2. Stochastic Implementation

Nakagami power is generated with the OMNeT++ Gamma random variate in Equation (3). The value returned to the channel engine is

$$A_{\text{Nakagami}} = 10 \log_{10}(P). \tag{5}$$

Consistently with the theoretical domain in Section 2.2, the implementation requires $m \geq 1/2$ and $\Omega > 0$. For both new models, the logarithm uses $\max(P, 10^{-12})$, preventing $-\infty$ or not-a-number values at zero or underflow while affecting only attenuation below -120 dB.

For the κ-μ process, node- and band-specific state preserves random phase, angle-of-arrival, and delay values across calls. To keep the cluster index consistent with the power expression below, the phase associated with cluster i is

$$\phi_i(t) = 2\pi[f_D \cos(\theta_i)t - f_c\tau_i], \qquad f_D = \frac{vf_c}{c}, \tag{6}$$

where v is vehicle speed, f_c is carrier frequency, and c is the speed of light. The implemented normalized instantaneous power is

$$P_{\kappa-\mu}(t) = \frac{1}{\mu(1+\kappa)} \sum_{i=1}^{\mu} \Big[\big(x_i(t) + \sqrt{\kappa}\cos\phi_i(t)\big)^2 + \big(y_i(t) + \sqrt{\kappa}\sin\phi_i(t)\big)^2 \Big], \tag{7}$$

where $x_i(t)$ and $y_i(t)$ are independent zero-mean Gaussian processes representing the in-phase and quadrature diffuse components of the ith cluster, respectively, with

$$x_i(t), y_i(t) \sim \mathcal{N}\left(0, \frac{1}{2}\right).$$

https://doi.org/10.3390/engproc2026158006

The returned fading value is $A_{\kappa\text{-}\mu}(t) = 10\log_{10} P_{\kappa\text{-}\mu}(t)$.

3.3. Verification Design and Evidence Boundaries

Verification has two stages. Stage 1 evaluates $m \in \{0.5, 1, 2, 3, 5\}$ with $\Omega = 1$ and $(\kappa, \mu) \in \{(0,1), (1,1), (2,1), (2,2), (2,4)\}$; the highlighted nominal settings $m = 2$, $\Omega = 1$, $\kappa = 2$, and $\mu = 2$ are retained for system-level simulations and quantitative outage/percentile comparisons.

Stage 2 examines basic, Rayleigh, Nakagami-m, and κ-μ exports for 1 and 100 vehicles over an approximately 1.2–1.8 km next-generation NodeB (gNB) distance interval and approximately 130/190 s traces. Outputs include uplink CQI and SINR, Radio Link Control (RLC) throughput and packet loss, and Medium Access Control (MAC) latency.

All cases use Max-CI; fading and common scheduling jointly shape SINR and throughput while preserving comparability.The main simulation parameters and retained configuration settings are summarized in Table 1.

Table 1. Reproducibility record for the retained simulations.

Item	Retained Value or Status
Fading configurations	Basic, Rayleigh, Nakagami-m, and κ-μ
Nominal fading parameters	$m = 2$, $\Omega = 1$, $\kappa = 2$, and $\mu = 2$
Vehicle load	1 and 100 vehicles
Displayed gNB distance interval	Approximately 1.2–1.8 km
Displayed time interval	Approximately 130 s (one vehicle) and 190 s (100 vehicles)
Carrier frequency and bandwidth	2.0 GHz carrier frequency, 20 MHz bandwidth (100 PRBs)
Vehicle speed and mobility model	50 km/h, `LinearMobility` model
Traffic model, packet size, and offered load	CBR UDP traffic, 1000-byte packet size, 10 ms packet interval
Scheduler and sampling rule	Max-CI (`maxCI`) scheduler, 1 ms TTI sampling rule
Random-number seeds	Default OMNeT++ seed configuration (`seed-set = 0`)

Table 2 records the software environment required for reproducibility.

Table 2. Software environment required to reproduce the simulations.

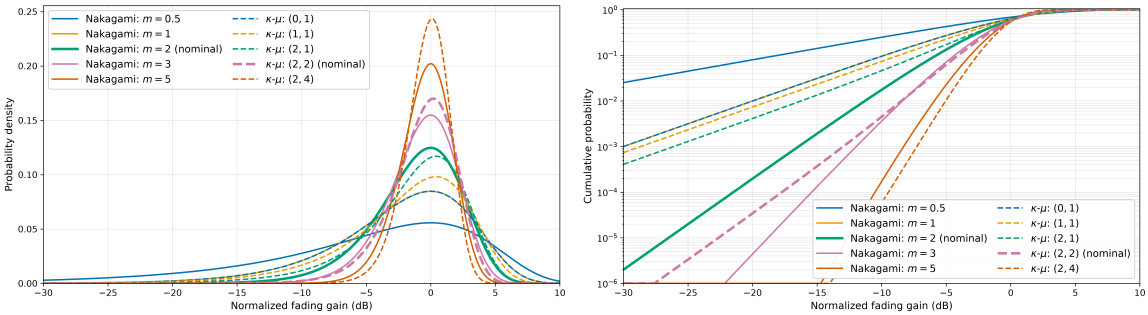
Software Component	Version Recorded in the Supplied Artifacts
Simu5G	Simu5G 1.5.0
OMNeT++	OMNeT++ 6.4.0
INET Framework	INET 4.7.0
Compiler	GCC 16.1.0
Operating system	Ubuntu 26.04 LTS

Because the archive lacks raw vectors and Stage 2 plotting scripts, these figures support trend/anomaly analysis rather than digitized estimates or confidence intervals. A title-excluded pixel test found identical plot bodies in all 12 3GPP/NR-labeled pairs; one file per pair is shown, and no 3GPP-versus-NR claim is made.

4. Results

4.1. Normalized Fading Distributions

Figure 1a shows broad Rayleigh/Jakes lower tails, greater concentration for Nakagami-m ($m = 2$), and the highest nominal concentration for κ-μ ($\kappa = 2$, $\mu = 2$). Jakes is a finite temporally correlated Rayleigh realization, included to expose temporal-process effects rather than as another marginal distribution.



(**a**) (**b**)

Figure 1. Normalized-power statistics for five parameter settings of each generalized-fading model. (**a**) Normalized fading gain distribution; (**b**) Outage-oriented CDF.

Figure 1 confirms that larger m, κ, or μ suppresses the corresponding lower tail; the Rayleigh-power cases $m = 1$ and $(\kappa, \mu) = (0, 1)$ coincide. For the highlighted nominal settings, outage at -10 dB is 0.0953, 0.0825, 0.0177, and 0.0045 for Rayleigh, Jakes, Nakagami-m, and κ-μ, respectively; at -5 dB it is 0.2718, 0.2512, 0.1329, and 0.0625. These parameter-specific results do not imply universal superiority.The corresponding normalized fading statistics, including the lower-tail probabilities and the 5th and 95th percentiles, are summarized in Table 3.

Table 3. Normalized fading statistics retained from the model-level verification.

Model	$P(G < -10\,\text{dB})$	$P(G < -5\,\text{dB})$	P5 (dB)	P95 (dB)
Rayleigh	0.0953	0.2718	−12.98	4.76
Jakes (SoS)	0.0825	0.2512	−12.40	4.59
Nakagami-m ($m = 2$)	0.0177	0.1329	−7.50	3.75
κ-μ ($\kappa = 2, \mu = 2$)	0.0045	0.0625	−5.43	2.97

4.2. Reference and Simulated SINR

In Figure 2, the basic single-vehicle trace follows the distance-dependent reference median, whereas Rayleigh, Nakagami-m, and κ-μ fluctuate mostly within its interval with isolated excursions. This verifies that the new options perturb, but preserve, the deterministic distance trend.

4.3. SINR and CQI Across Distance

Figure 3a,b retain the distance trend with greater stochastic variation. Mean uplink SINR for Basic, Rayleigh, Nakagami-m, and κ-μ is -4.4534, -8.4315, -7.6898, and -10.5500 dB for one vehicle and -4.6626, -3.4345, -5.5270, and -4.7772 dB for 100 vehicles.

CQI decreases with distance in the basic case and switches among adjacent levels under fading. Its narrow range and unavailable modulation-and-coding mapping make it less discriminating than SINR, so the CQI plots are omitted.

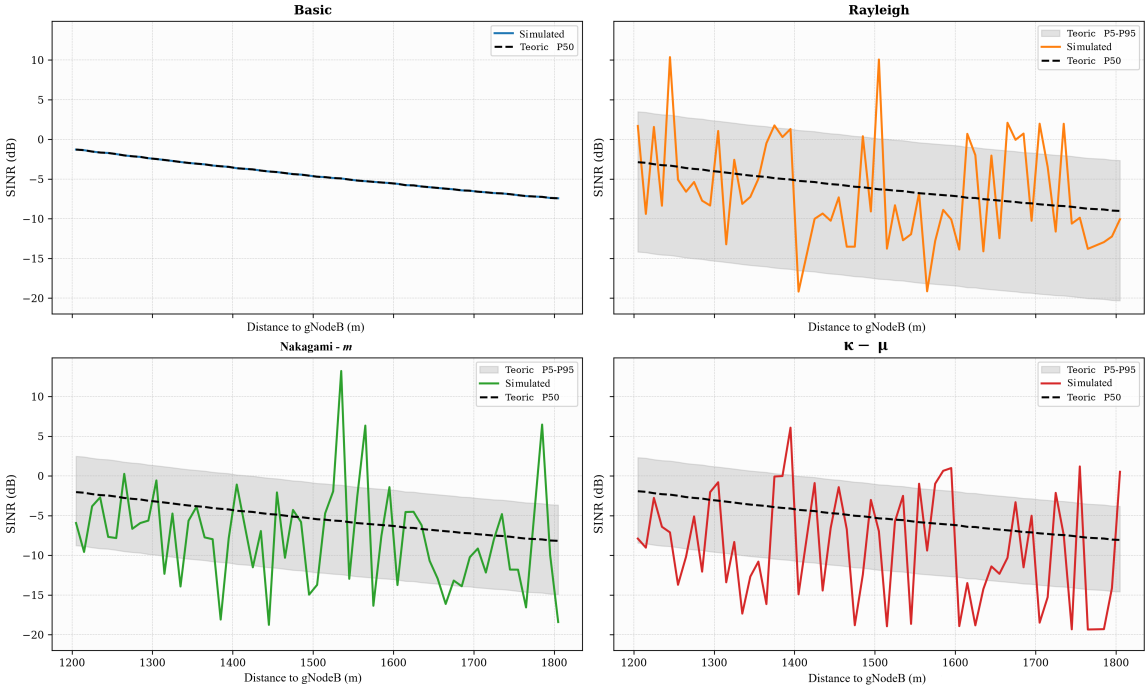
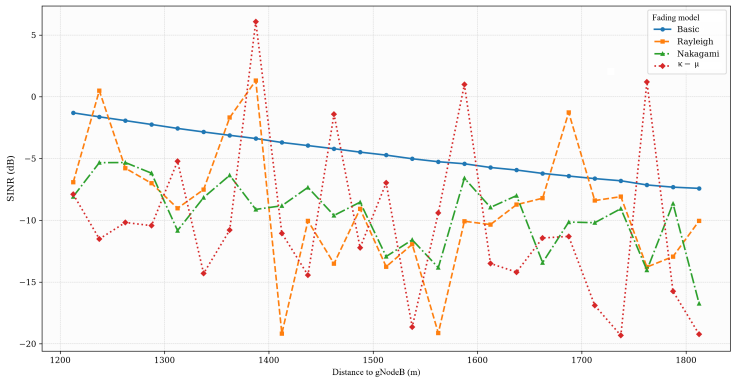
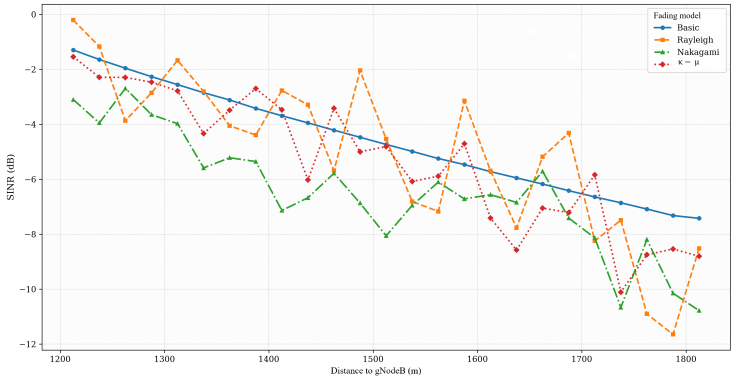


Figure 2. Reference and simulated uplink SINR for the retained single-vehicle export.



(**a**)



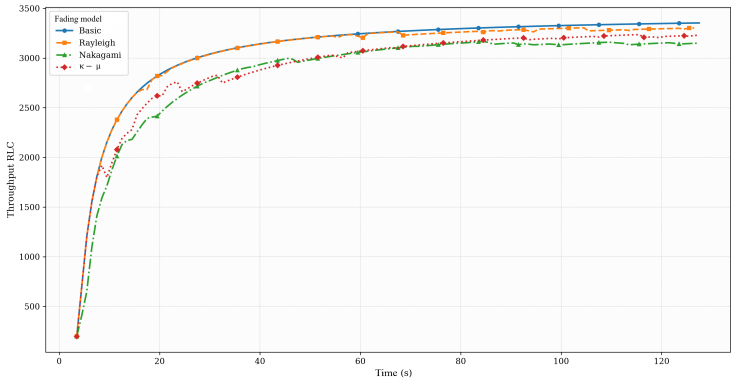
(**b**)

Figure 3. Uplink SINR versus gNB distance for the retained simulation exports. (**a**) Single-vehicle retained export; (**b**) 100-vehicle retained export.

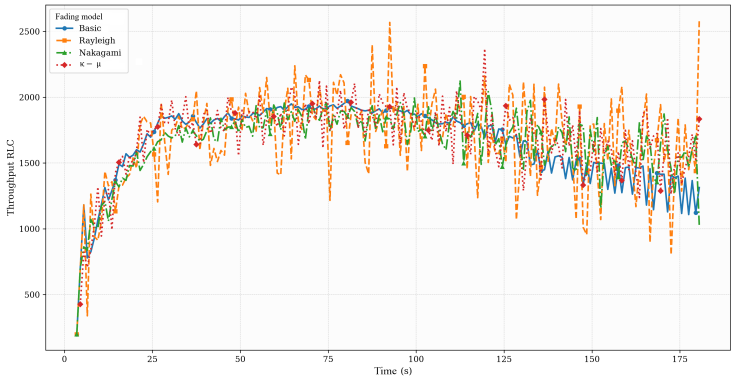
https://doi.org/10.3390/engproc2026158006

4.4. RLC Throughput Under Vehicle Load

Figure 4a reaches a plateau after an initial ramp, with mean RLC uplink throughput of 3094.52, 3065.83, 2885.87, and 2929.16 B/s for Basic, Rayleigh, Nakagami-m, and κ-μ. The more variable 100-vehicle traces in Figure 4b yield per-vehicle means of 1265.12, 1220.87, 1251.27, and 1272.25 B/s.



(**a**)



(**b**)

Figure 4. RLC uplink throughput versus time for the retained simulation exports. (**a**) Single-vehicle retained export; (**b**) 100-vehicle retained export.

5. Discussion

The extension broadens channel conditions without changing `fadingType`; m, Ω, κ, and μ enable controlled sensitivity studies. Normalized verification confirms the expected tail ordering but not automatic end-to-end improvement.

System outputs combine fading, distance, interference, scheduling, traffic, and protocol state: no model dominates throughput at every instant, and generalized models can show deep SINR excursions despite lighter normalized tails. The supported claim is therefore greater modeling expressiveness and verified integration, not universal performance gains.

The sweep demonstrates flexibility, while the nominal set preserves control. Future work includes broader V2X campaigns, regression tests, examples, version checks, and upstream Simu5G review.

6. Conclusions

Configurable Nakagami-m and κ-μ fading was integrated into Simu5G channel and background-interference workflows while preserving NED/INI configuration. Five settings per model confirm parameter sensitivity; nominal cases reduce deep-fading probability rela-

tive to Rayleigh/Jakes. Single-vehicle and 100-vehicle exports verify propagation into SINR, CQI, throughput, latency, and packet loss without implying uniform network-level gains.

The audited artifacts support a traceable, configurable generalized-fading extension for 5G vehicular studies; future system-level campaigns will cover additional parameters and V2X conditions.

Author Contributions: Conceptualization, R.M.V. and J.R.V.; methodology, R.M.V. and J.R.V.; software, J.R.V.; validation, L.U.-A., J.V.-S. and M.A.I.; formal analysis, L.U.-A.; investigation, R.M.V. and J.R.V.; writing—review and editing, L.U.-A. and M.A.I.; supervision, M.A.I. All authors have read and agreed to the published version of the manuscript.

Funding: This research was supported by the research project PIGR-24-02, 'SmartCityNet: IoT y Redes Vehiculares para la Optimización y Transformación Urbana', funded by Escuela Politécnica Nacional, and by Project DISCOVERY (PID2023-148716OB-C32), funded by the Ministerio de Ciencia e Innovación, Spain.

Institutional Review Board Statement: Not applicable.

Informed Consent Statement: Not applicable.

Data Availability Statement: The public GitHub archive (https://github.com/RicardoMena187/PaperNakagamiKappa, accessed on 15 July 2026) provides the retained result figures, SHA-256 manifest, scenario and metric dictionary, and citation metadata, preserving the provenance and nominal configuration of the reported evaluation.

Conflicts of Interest: The authors declare no conflicts of interest.

References

1. Nardini, G.; Sabella, D.; Stea, G.; Thakkar, P.; Virdis, A. Simu5G: An OMNeT++ Library for End-to-End Performance Evaluation of 5G Networks. *IEEE Access* **2020**, *8*, 181176–181191. [CrossRef]
2. Nardini, G.; Stea, G.; Virdis, A.; Sabella, D. Simu5G: A System-level Simulator for 5G Networks. In *Proceedings of the 10th International Conference on Simulation and Modeling Methodologies, Technologies and Applications*; SCITEPRESS: Setúbal, Portugal, 2020; pp. 68–80. [CrossRef]
3. Molisch, A.F.; Tufvesson, F.; Karedal, J.; Mecklenbräuker, C.F. A Survey on Vehicle-to-Vehicle Propagation Channels. *IEEE Wirel. Commun.* **2009**, *16*, 12–22. [CrossRef]
4. Mecklenbräuker, C.F.; Molisch, A.F.; Karedal, J.; Tufvesson, F.; Paier, A.; Bernadó, L.; Zemen, T.; Klemp, O.; Czink, N. Vehicular Channel Characterization and Its Implications for Wireless System Design and Performance. *Proc. IEEE* **2011**, *99*, 1189–1212. [CrossRef]
5. Jakes, W.C. (Ed.) *Microwave Mobile Communications*; Wiley: New York, NY, USA, 1974.
6. Pätzold, M.; Laue, F. Statistical Properties of Jakes' Fading Channel Simulator. In *Proceedings of the 48th IEEE Vehicular Technology Conference*; IEEE: New York, NY, USA, 1998; pp. 712–718.
7. Fulghum, T.; Molnar, K.; Duel-Hallen, A. *The Jakes Fading Model for Antenna Arrays Incorporating Angular Spread*; Technical Report TR-1997-13; North Carolina State University: Raleigh, NC, USA, 1997.
8. Nakagami, M. The *m*-Distribution: A General Formula of Intensity Distribution of Rapid Fading. In *Statistical Methods in Radio Wave Propagation*; Hoffman, W.C., Ed.; Pergamon Press: Oxford, UK, 1960; pp. 3–36.
9. Yacoub, M.D. The κ-μ Distribution and the η-μ Distribution. *IEEE Antennas Propag. Mag.* **2007**, *49*, 68–81. [CrossRef]
10. Naik, G.; Choudhury, B.; Park, J.M. IEEE 802.11bd and 5G NR V2X: Evolution of Radio Access Technologies for V2X Communications. *IEEE Access* **2019**, *7*, 70169–70184. [CrossRef]
11. Emara, M.; Filippou, M.C.; Sabella, D. MEC-Assisted End-to-End Latency Evaluations for C-V2X Communications. In *Proceedings of the European Conference on Networks and Communications*; IEEE: New York, NY, USA, 2018; pp. 1–9.
12. Nardini, G.; Noferi, A.; Ducange, P.; Stea, G. Exploiting Simu5G for Generating Datasets for Training and Testing AI Models for 5G/6G Network Applications. *SoftwareX* **2023**, *21*, 101320. [CrossRef]
13. Kovács, G.A.; Bokor, L. Implementation of MEC-Assisted Collective Perception in an Integrated Artery/Simu5G Simulation Framework. *Sensors* **2023**, *23*, 7968. [CrossRef] [PubMed]
14. Rehman, A.; Valentini, R.; Cinque, E.; Di Marco, P.; Santucci, F. On the Impact of Multiple Access Interference in LTE-V2X and NR-V2X Sidelink Communications. *Sensors* **2023**, *23*, 4901. [CrossRef] [PubMed]

15. Guo, J.; Zhang, D.; You, L.; Zhang, X.; Mumtaz, S. SER Performance Analysis of Generalized κ-μ and η-μ Fading Channels. *J. Commun. Netw.* **2024**, *26*, 193–206. [CrossRef]
16. Wang, H.; Xu, G.; Liu, J.; Song, Z.; Zhang, Q.; Zhang, W. The λ–κ–μ Fading Distribution. *IEEE Antennas Wirel. Propag. Lett.* **2024**, *23*, 4398–4402. [CrossRef]
17. Liu, J.; Xu, G.; Wang, H.; Zhang, C.; Lu, X. Double λ-κ-μ Distribution: Modeling and Performance Evaluation in Non-Homogeneous Environments. *IEEE Wirel. Commun. Lett.* **2025**, *14*, 3378–3382. [CrossRef]
18. Upaddhyay, V.K.; Soni, S.K.; Chauhan, P.S. The α-η-μ/Inverse Gamma Fading Subjected to Wireless Applications with MRC Diversity. *Int. J. Commun. Syst.* **2022**, *35*, e5102. [CrossRef]
19. Wang, H.; Liu, J.; Zhang, C.; Yang, Z.; Xu, G. Log-λ-κ-μ Distribution: A New Channel Model for Low-Altitude UAV Communications. *IEEE Trans. Veh. Technol.* **2026**, *Early Access*. [CrossRef]
20. 3GPP. *Study on Channel Model for Frequencies from 0.5 to 100 GHz*; Technical Report TR 38.901, 3rd Generation Partnership Project; 3GPP: Sophia Antipolis, France, 2020.
21. 3GPP. *NR and NG-RAN Overall Description; Stage 2*; Technical Specification TS 38.300, 3rd Generation Partnership Project; 3GPP: Sophia Antipolis, France, 2020.

Disclaimer/Publisher's Note: The statements, opinions and data contained in all publications are solely those of the individual author(s) and contributor(s) and not of MDPI and/or the editor(s). MDPI and/or the editor(s) disclaim responsibility for any injury to people or property resulting from any ideas, methods, instructions or products referred to in the content.